OBSTETRICS

Immune tolerance attenuates gut dysbiosis, dysregulated uterine gene expression and high-fat diet potentiated preterm birth in mice

Clarence R. Manuel, PhD; Mariam S. Latuga, MD; Charles R. Ashby Jr, PhD; Sandra E. Reznik, MD, PhD

BACKGROUND: Preterm delivery accounts for 85% of perinatal morbidity and mortality. Although the consumption of a high-fat diet leads to exaggerated proinflammatory responses and, in pregnant women, increased rates of spontaneous preterm birth, the underlying mechanisms remain unclear.

OBJECTIVE: We sought to elucidate the mechanisms by which maternal consumption of a high-fat diet leads to a dysregulated immune response and, subsequently, spontaneous preterm birth.

STUDY DESIGN: We performed 16S ribosomal RNA sequencing of DNA extracted and amplified from stool samples and compared the gut microbiomes of lipopolysaccharide-induced pregnant mice that were maintained on a high-fat diet compared to a normal control diet. Next, we sequenced the uterine transcriptomes of the mice. To test the effect of dampening of the immune response on the microbiome, transcriptome, and risk of spontaneous preterm birth, we induced immune tolerance with repetitive subclinical doses (0.2 mg/kg/week for 8 weeks) of endotoxin and performed 16S ribosomal RNA and uterine transcriptome sequencing on these immunotolerized mice.

RESULTS: High-fat diet potentiates lipopolysaccharide-induced preterm birth by affecting the maternal gut microbiome and uterine transcriptome and reduces antioxidant capacity in a murine model. High-fat diet consumption also increases the colonization of the gut by 5 immunogenic bacteria and decreases colonization by *Lachnospiraceae_NK4A136_group*. Uteri from high-fat diet mice had increased expression of genes that stimulate the inflammatory-oxidative stress axis, autophagy/apoptosis, and smooth muscle contraction. Repetitive endotoxin priming protects high-fat diet dams from spontaneous preterm birth, increases colonization of the gut by *Lachnospiraceae_NK4A136_group*, decreases levels of immunogenic bacteria in the gut microbiome, and reduces the number of dysregulated genes after high-fat diet consumption from 994 to 74.

CONCLUSION: High-fat diet-potentiated spontaneous preterm birth is mediated by increased inflammation, oxidative stress, and gut dysbiosis. The induction of immune tolerance via endotoxin priming reverses these effects and protects high-fat diet dams from spontaneous preterm birth. Based on this work, the role of immunomodulation as a novel therapeutic approach to prevent preterm birth among women who consume high-fat diets should be explored.

Key words: endotoxin, immune tolerance, microbiome, preterm birth, priming

Preterm births occur at <37 weeks of gestation and are the leading cause of neonatal morbidity and death worldwide.[1] Each year, an estimated 15 million babies are born preterm.[2] Complications from these deliveries adversely affect the mother and newborn infant. For example, preterm babies are at higher risk of the development of neurologic, respiratory, and metabolic abnormalities.[3] Currently, the only approved drug in the United States that delays preterm deliveries is the progesterone analog 17-hydroxyprogesterone caproate (17-OHPC). Unfortunately, the efficacy of 17-OHPC is variable, and it does not delay active preterm deliveries.[4,5] Also, 17-OHPC lacks efficacy in the following groups: (1) women with multiple fetuses, (2) obese women, and (3) women with short cervix and it is not appropriate for women who have no history of spontaneous preterm birth (sPTB). In a retrospective cohort, rates of sPTB were still high among African American women who were treated with 17-OHPC. The lack of or variable response in obese and African American women is problematic because 1 in 4 pregnant women are overweight or obese and because they are at the highest risk of having a preterm delivery.[6,7]

Although maternal infection was previously believed to be the most significant risk factor for sPTB, recent studies demonstrate that maternal infection is not required in spontaneous preterm deliveries.[8] Additionally, PTB is a multifactorial syndrome that may result from sterile inflammation, oxidative stress, dysbiosis of maternal microbiome, and secretion of exosomes.[8-10] Furthermore, epidemiologic studies demonstrate that environmental factors, such as maternal diet, are correlated with sPTB.[11-18]

Despite the significant clinical correlation between high-fat diet (HFD) consumption and sPTB, it remains unknown as to how a HFD increases the risk of spontaneous preterm delivery. Here, we report that HFD consumption potentiates inflammation and initiates spontaneous preterm delivery by disrupting immune tolerance, increasing oxidative stress, and altering the maternal gut microbiome and uterine transcriptome.

Lipopolysaccharide (LPS) is an endotoxin that is secreted from Gram-negative bacteria that stimulates the toll-like receptor 4 (TLR4).[19] The activation of TLR4 in the uteroplacental environment induces the production of cytokines, chemokines, and reactive

Cite this article as: Manuel CR, Latuga MS, Ashby CR Jr, et al. Immune tolerance attenuates gut dysbiosis, dysregulated uterine gene expression and high-fat diet potentiated preterm birth in mice. Am J Obstet Gynecol 2019;220:596.e1-28.

0002-9378/$36.00

https://doi.org/10.1016/j.ajog.2019.02.028

AJOG at a Glance

Why was this study conducted?
Consumption of a high-fat diet potentiates lipopolysaccharide-induced preterm birth in mice.

Key findings
A high-fat diet leads to gut dysbiosis and dysregulated uterine gene expression in pregnant mice.

What does this add to what is known?
The induction of immune tolerance partially reverses the effects of high-fat diet consumption in pregnant mice.

oxygen species.[8,20-22] This milieu of inflammatory and free radical–producing species may induce labor.[8] In this study, we hypothesized that repetitive dosing (ie, priming) of HFD mice with LPS would decrease rates of spontaneous preterm delivery by decreasing inflammation/oxidative stress. We further hypothesized that the immune tolerance produced by LPS priming would normalize the maternal gut microbiome and uterine transcriptome.

Materials and Methods

Experimental design

Eight-week-old female C57Bl/6 mice were purchased from Jackson Laboratories (Bar Harbor, ME). All procedures complied with the St. John's University Institutional Animal Care and Use Committee. Research was conducted according to the National Institutes of Health Guide for the Care and Use of Laboratory Animals, eighth edition, National Research Council (US) Committee for the Update of the Guide for the Care and Use of Laboratory Animals. Mice were housed at 24°C on a day and night cycle of 12 hours each. Animals had ad libitum access to food and water.

In our in vivo study, 8-week old female mice were assigned randomly to 4 groups. After acclimating mice to the Animal Care Center for 12–14 days, group 1 consumed a normal control diet (NCD; Diet 5001, Lab Diet, Lab Animal, St Louis, MO) and group 2 consumed a HFD that contained 60% fat (Diet 58Y1, TestDiet, Lab Animal, St Louis, MO) for 8 weeks and during pregnancy. Group 3 followed the same diet regimen as group 1 but also received a subclinical dose (0.2 mg/kg intraperitoneally) of LPS (*Escherichia coli* O111:B4; Sigma-Aldrich, St Louis, MO) once per week for 8 weeks, and on E1 and E8 of gestation. Group 4 followed the same diet regimen as group 2 but also received the same subclinical doses of LPS as group 3. On day E15.5, groups 1–4 received a bolus dose of LPS (0.3 mg/kg intraperitoneally), and the onset time of delivery and fetal viability were monitored.

Intraperitoneal glucose and insulin tolerance tests

To determine the sensitivity of glucose and insulin-responsive tissues in mice, we measured glucose level in blood over time after a bolus intraperitoneal injection of glucose (Sigma) or insulin (Humalin R; Eli Lilly, Indianapolis, IN). At the beginning and conclusion of the 8 week NCD or HFD regimen, mice were fasted for 8 hours; food was taken away early in the morning (7:00 AM). For the intraperitoneal glucose tolerance tests, we measured fasting glucose levels at T=0 and after administering glucose (2 g/kg) at T=15, 30, 60, and 120 minutes. For the intraperitoneal insulin tolerance tests, we measured fasting glucose levels at T=0 and after administering insulin (0.5 U/kg) at T=15, 30, 45, 60, and 120 minutes. Glucose and insulin solutions were prepared in sterile 1X phosphate buffered saline solution. Blood was collected by tail snip with a scalpel and gentle massage of the tail. A calibrated glucose meter and test strips (Alpha-TRAK2; ADW Diabetes, Pompano Beach, FL) were used to measure circulating glucose levels.

Food consumption and weight gain

After initiation of the NCD or HFD 8-week regimen, food consumption and weight were measured weekly. Mice were housed individually and provided 40 grams of NCD or HFD pellets at the beginning of each week for a total of 8 weeks. Mice had ad libitum access to food and water. We determined food consumption by reweighing food pellets at the end of each week. We determined weight gain by weighing mice in the morning 1 time per week for a total of 8 weeks.

Bodily fluid and tissue collection

At the beginning and end of the 8-week NCD or HFD regimen, urine was collected with special non-absorbent bedding (LabSand, Braintree Scientific, Inc, Braintree, MA). In the morning (7:00 AM), mice were singly housed, and standard bedding was replaced with one-half a bag of LabSand. Urine was collected with a plastic transfer pipette and centrifuged at 1500 rpm for 5 minutes to remove particles from urine samples. After centrifugation, urine samples were immediately stored at −80°C. Stool samples were collected on the same day as urine samples. Mice were singly housed, and stools were collected at the end of the day (4:00 PM). Upon collection, stools were immediately stored at −80°C.

We collected serum samples after dams delivered their first pups. Sera were collected by cardiac puncture. During cardiac puncture, mice were anesthetized briefly with isoflurane gas (3%), and blood was drawn from the heart with a 1-mL syringe and 23-gauge needle. Sera were collected in Z serum clot activator tubes (Greiner Bio-One, Greiner Bio-One North America Inc, Monroe, NC), and we followed the manufacturer's instructions to isolate sera from plasma. On collection, sera were stored at −80°C. Uteri and placenta

FIGURE 1
High-fat diet consumption impairs glucose and insulin tolerance

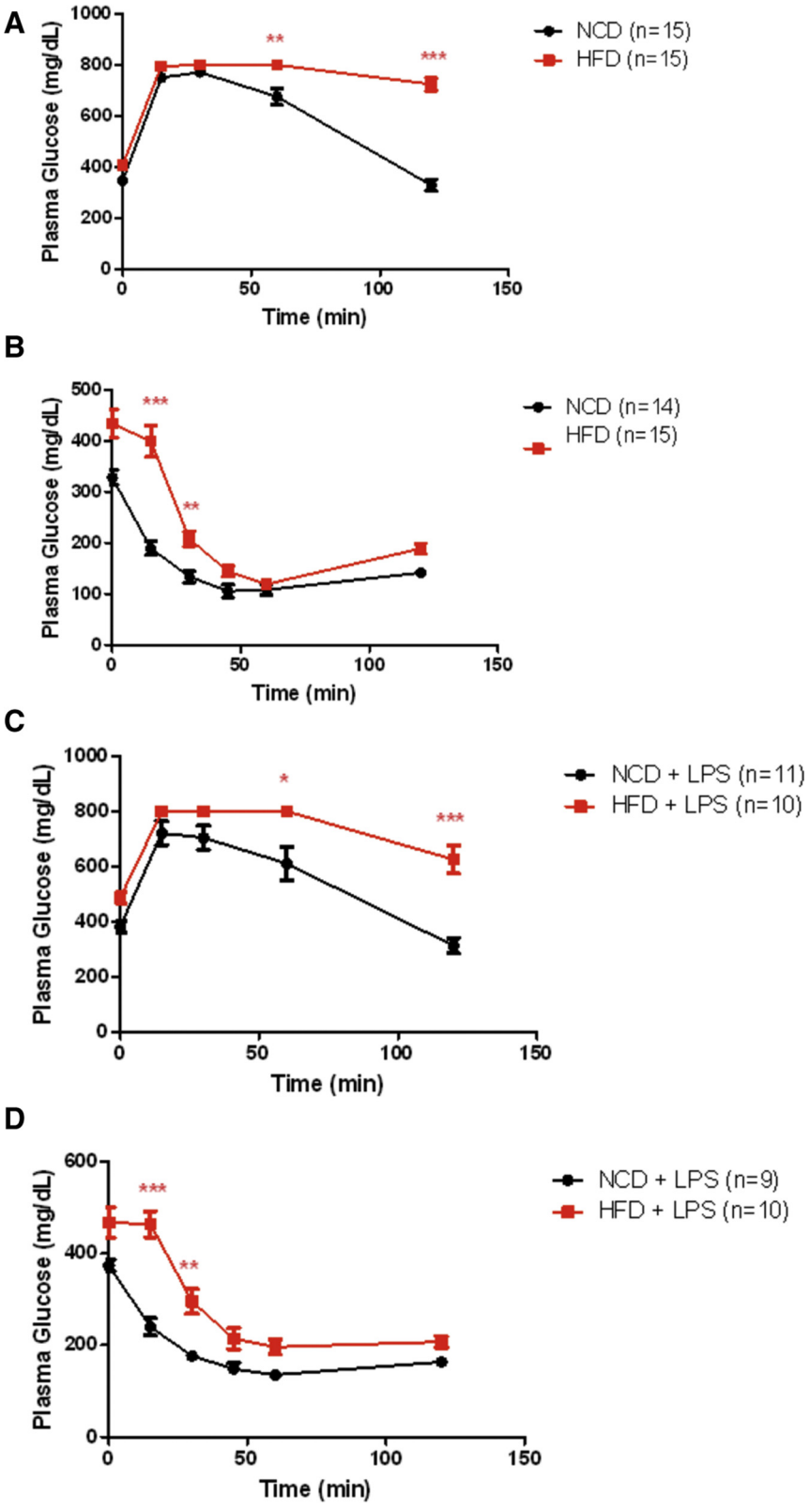

A, Intraperitoneal glucose tolerance test in the normal control diet and high-fat diet groups. Plasma glucose levels were determined at T=0, 15, 30, 60, and 120 minutes. **B,** Intraperitoneal insulin tolerance test in the normal control diet and high-fat diet groups. Plasma glucose levels were recorded at T=0, 15, 30, 45, 60, and 120 minutes. **C,** Intraperitoneal glucose tolerance test in normal control diet and high-fat diet—lipopolysaccharide-primed groups. Plasma glucose levels were determined at T=0, 15, 30, 60, and 120 minutes. **D,** Intraperitoneal insulin tolerance test in normal control diet and high-fat diet—lipopolysaccharide-primed groups. Plasma glucose levels were determined at T=0, 15, 30, 60, and 120 minutes. The *asterisk* denotes $P<.05$; the *double asterisks* denote $P<.01$; the *triple asterisks* denote $P<.001$.

HFD, high-fat diet; *LPS*, lipopolysaccharide; *NCD*, normal control diet.

Manuel et al. Immune tolerance decreases risk of preterm birth in high-fat diet mice. Am J Obstet Gynecol 2019.

were harvested during necropsy after dams delivered their first pups and immediately were stored in RNAlater solution (Qiagen, Germantown, MD) for 24 hours at −20°C. The uteri and placenta were then stored at −80°C.

Oxidative stress and inflammation assays

To assess oxidative stress, we collected urine and sera and performed total antioxidant capacity (Cell BioLabs, San Diego, CA) and the thiobarbituric acid reactive substances (Cayman Chemical, Ann Arbor, MI) assays. The total antioxidant capacity assay measures antioxidant capacity based on reduction of copper (II) to copper (I), and the number of copper-reducing equivalents (Cayman Chemical). The thiobarbituric acid reactive substances assay measures malondialdehyde production, a marker of lipid peroxidation (Cayman Chemical). Sera were used in the total antioxidant capacity assay, and urine samples were used in the thiobarbituric acid reactive substances assay. Both oxidative stress assays were performed as described by the manufacturers.

To assess inflammation, we prepared tissue homogenates of uteri and measured a p38 mitogen activated protein kinase (MAPK) activation (Thermo Fisher, Franklin, MA). Briefly, uteri were lysed in radio immunoprecipitation assay lysis buffer (G Biosciences, St Louis, MO), freshly supplemented

FIGURE 2
High-fat diet—lipopolysaccharide-primed mice consume less food than high-fat diet mice

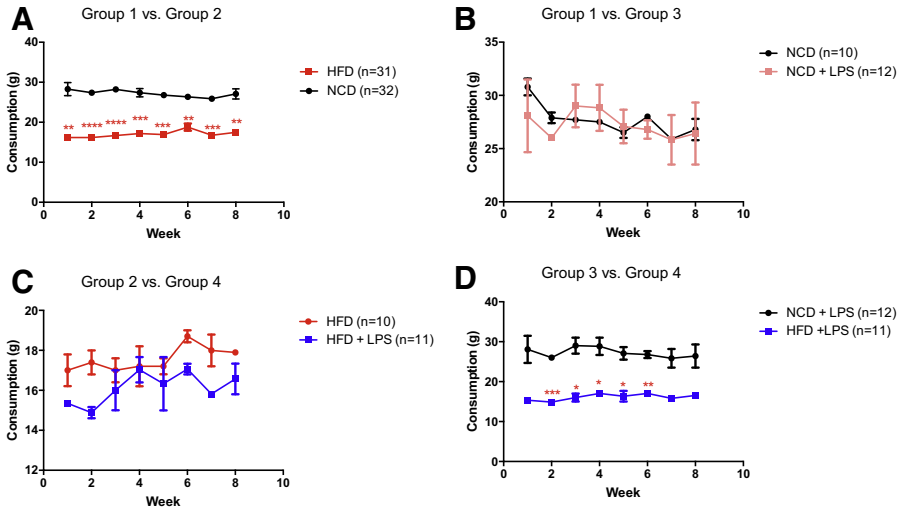

Food consumption was measured once per week for 8 weeks total. **A,** Food consumption in normal control diet and high-fat diet groups. **B,** Food consumption in normal control diet and normal control diet—lipopolysaccharide—primed groups. **C,** Food consumption in high-fat diet and high-fat diet—lipopolysaccharide-primed groups. **D,** Food consumption in normal control diet— and high-fat diet—lipopolysaccharide-primed groups.

*$P<.05$; **$P<.01$; ***$P<.001$; ****$P<.0001$ *HFD*, high-fat diet; *LPS*, lipopolysaccharide; *NCD*, normal control diet.

Manuel et al. Immune tolerance decreases risk of preterm birth in high-fat diet mice. Am J Obstet Gynecol 2019.

before use with 1 mmol/L of phenylmethylsulfonylfluoride and ethylenediaminetetraacetic acid-free protease inhibitor cocktail set III (Calbiochem, St Louis, MO). Uteri were homogenized on ice with the use of a polytron homogenizer (Lauda-BrinkMann, Delran, NJ) by repeated homogenization every 20 seconds for 3 intervals. Samples were then centrifuged at 14,000*g* for 20 minutes at 4°C, and supernatants were collected as lysates. Protein concentrations of the samples were determined with the bicinchoninic acid protein assay (Thermo Fisher). The manufacturer's instructions were followed to determine p38 MAPK activation in collected lysates.

Progesterone assay

To determine the circulating levels of progesterone, we measured progesterone using a competitive colorimetric enzyme-linked immunosorbent assay (Cayman Chemical). The manufacturer's instructions were followed to perform the assay.

16S ribosomal RNA sequencing of stool samples and analyses

To evaluate the diversity of gut microbiota, we sent stool samples to CD Genomics (Shirley, NY) for 16S ribosomal RNA (16S RNA) sequencing. CD Genomics performed the following procedures: genomic DNA extraction, polymerase chain reaction amplification and purification, and DNA library construction and sequencing. Illumina HiSeq PE250 strategy was used for 16S RNA sequencing, and V3—V4 variable regions (primer set 341F and 806R) were targeted.

In this project, 1,678,981 pair-end reads were obtained for 21 samples in total; after pair-end reads merging and filtering, 1,129,512 clean tags were generated, which was an average of 79,951 clean tags for each sample. Amplicons were processed using a paired-end Illumina HiSeq2500 platform to generate 250 base pair paired-end raw reads and then pretreated. Paired-end reads were assigned to a sample by their unique barcode, and the barcode and primer sequence were then truncated. Paired-end reads were merged with the use of fast length adjustment of short reads (V1.2.7,http://ccb.jhu.edu/software/FLASH/), which is a fast and accurate analysis tool to merge pairs of reads when the original DNA fragments are shorter than twice of the reads length. The obtained splicing sequences were called "raw tags." Quality filtering was then performed on the raw tags under specific filtering conditions of Trimmomatic (version 0.33, Usadel Lab, Aachen, Germany; http://www.usadellab.org/cms/?page=trimmomatic) quality control process. After the tags were filtered, high-quality clean tags were obtained. The tags were compared with the reference database (Gold database; http://drive5.com/uchime/uchime_download.html) with the UCHIME algorithm (UCHIME Algorithm http://www.drive5.com/usearch/manual/uchime_algo.html) to detect chimeric sequences; then the chimeric sequences were removed.

UCLUST in QIIME (version 1.8.0) was used to cluster the tags with 97% similarity and acquired the operational taxonomic units (OTUs). Then, OTUs were annotated based on the Silva taxonomic database (Max Planck Institute for Marine Microbiology and Jacobs University, Bremen, Germany). At the level of 97% similarity, we obtained the OTU number for each sample. The OTUs annotated as mitochondria, chloroplast, and unknown were removed. To assess species annotation resolution ratio of OTUs and species complexity for each sample, the statistical amount of sequences of every sample in each classification level (Kingdom, Phylum, Class, Order, Family, Genus, and Species) was calculated. The abundance of information in each taxonomic level was generated with QIIME, and the microbial community structure graphs of each level were drawn by R language tool.

Phylogenetic Investigation of Communities by Reconstruction of Unobserved States (PICRUSt) software (Free Software Foundation, Boston, MA) was used to characterize the functional genes in the sample by a comparison of the

FIGURE 3
High-fat diet—lipopolysaccharide-primed mice gain less weight than high-fat diet mice

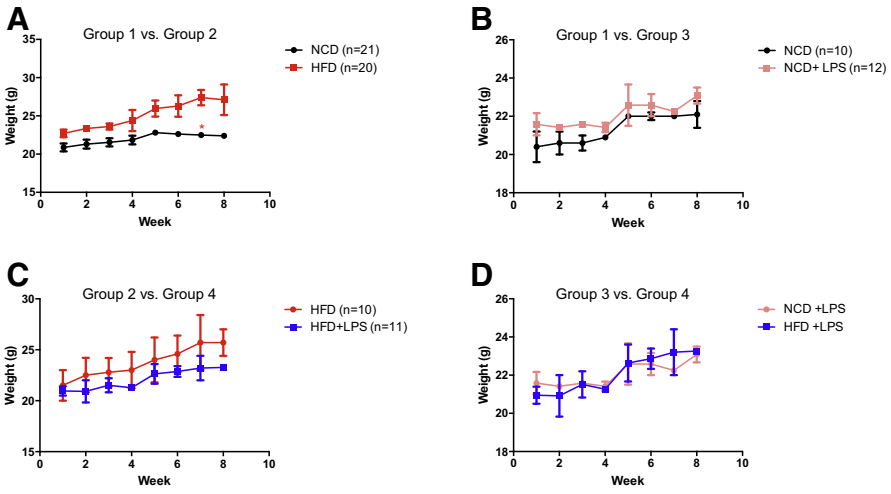

Weight gain was measured once per week for 8 weeks total. **A,** Weight gain in normal control diet and high-fat diet groups. **B,** Weight gain in high-fat diet and high-fat diet—lipopolysaccharide-primed groups. **C,** Weight gain in normal control diet and normal control diet—lipopolysaccharide-primed groups. **D,** Weight gain in normal control diet— and high-fat diet—lipopolysaccharide-primed groups.

*$P<.05$; *HFD*, high-fat diet; *LPS*, lipopolysaccharide; *NCD*, normal control diet.

Manuel et al. Immune tolerance decreases risk of preterm birth in high-fat diet mice. Am J Obstet Gynecol 2019.

bacterial composition information that was obtained from the 16S sequencing data. First, we standardized the generated OTUs, then through the corresponding green gene identification of each OTU, we obtained the related Kyoto Encyclopedia of Genes and Genomes and Cluster of Orthologous Group family information, the abundance of these Kyoto Encyclopedia of Genes and Genomes and Cluster of Orthologous Group families was calculated. Next, we used G-test in Statistical Analysis of Metagenomic Profiles (STAMP) and Fisher exact test for the species abundance at genus level to perform the significant difference test between 2 samples and *t*-test between 2 groups. The a priori probability value was .05.

Uterus RNA transcriptome analyses

To evaluate the RNA transcriptome of uteri, we sent uteri to CD Genomics for RNA-sequencing. CD Genomics performed the following procedures: RNA extraction, enrichment of messenger RNA, complementary DNA conversion, library preparation, and sequencing. Illumina HiSeq PE150 strategy was used for RNA sequencing, and Illumina HiSeq strategy SE50 was used for differential gene expression (Illumina Inc, San Diego, CA).

The source of reference genome information was http://www.ensembl.org/Mus_musculus/Info/Index. Tophat2 (a bioinformatics package that aligns RNA sequences with insertions, deletions, and fusion breaks) mapped filtered sequences to the reference genome. Clean reads were aligned with the reference genome to obtain positional information on the reference genome or gene and sequence characteristic information that was unique to the sequencing sample. We used Cuffquant and Cuffnorm components of Cufflinks software (version 1; Trapnell Lab, Seattle, WA) to quantify transcripts and gene expression levels with the use of mapped reads positional information on the gene. The number of differentially expressed genes (DEGs) and the expression level of each single gene were analyzed.

DESeq (differential expression analysis for sequence count data) was used to analyze the DEGs for samples with biologic replicates; EBSeq (differential expression analysis for genes and their isoforms) was used for samples without replicates. During the process, fold change ≥ 2 and false discovery rate <0.01 were set as screening criteria. Fold change indicates the ratio of expression levels between 2 samples (groups). The false discovery rate was obtained by correcting the probability value of the significant difference. The Benjamini-Hochberg calibration method was used for the differential expression analysis. The probability value that was obtained from the test was corrected, and the false discovery rate was used as a key indicator of DEGs.

Statistical analyses

The data from the in vivo study, where mice consumed either a NCD or HFD for 8 weeks and during pregnancy, were analyzed using GraphPad Prism software (version 6; Graphpad Software, San Diego, CA). For the intraperitoneal glucose tolerance tests and intraperitoneal insulin tolerance tests data, we performed a paired, 2-tailed Student *t* test. We evaluated food consumption and weight gain using an unpaired 2-tailed Student *t* test. To assess sPTB outcomes between NCD and HFD mice, we performed a 1-sided chi-square test. We used a 1-way analysis of variance to evaluate sPTB outcomes across all groups. Post hoc analysis, after analysis of variance, was performed with the Bonferroni's multiple comparison test to test for significant differences in rates of sPTB. Last, we analyzed the circulating progesterone, oxidative stress, and inflammation data using a 1-way analysis of variance, followed by Tukey's post hoc analysis, to evaluate differences in progesterone and measures of oxidative stress and Newman-Keuls multiple comparison tests to discern differences in levels of p38 MAPK activation. The a priori probability value was set at $<.05$.

FIGURE 4
High-fat diet consumption potentiates lipopolysaccharide-induced preterm birth; lipopolysaccharide priming protects high-fat diet mice from spontaneous preterm birth

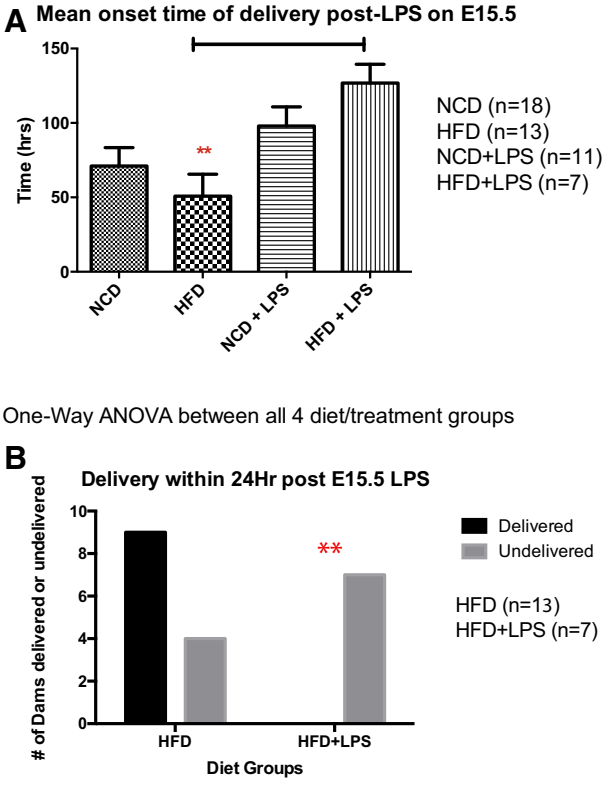

A, Mean onset of delivery in groups 1–4. Statistical significance was determined with the use of the Bonferroni multiple comparison test after 1-way analysis of variance (**$P<.01$). **B**, Delivered or undelivered high-fat diet dams with or without priming after lipopolysaccharide exposure on E15.5 (**$P<.01$).

HFD, high-fat diet; *LPS*, lipopolysaccharide; *NCD*, normal control diet.

Manuel et al. Immune tolerance decreases risk of preterm birth in high-fat diet mice. Am J Obstet Gynecol 2019.

Results

Priming HFD mice with LPS partially reverses HFD-induced alterations in metabolism

To evaluate glucose and insulin tolerance, we performed intraperitoneal glucose and insulin tolerance tests and found that HFD mice have impaired glucose and insulin tolerance compared with NCD mice (Figure 1, A and B). Priming with LPS (0.2 mg/kg/week x 8 weeks), did not significantly improve the glucose or insulin tolerance of HFD mice compared to NCD mice (Figure 1, C and D). However, HFD-LPS–primed mice consumed less food and gained less weight over the course of the diet regimen compared with HFD mice (Figures 2 and 3).

HFD consumption potentiates LPS-induced PTB

To further explore the relationship between HFD and PTB and to investigate the mechanisms of HFD-induced PTB, we designed the first in vivo model of HFD-potentiated PTB. In our model, we used LPS, a Gram-negative endotoxin, to stimulate inflammation. LPS is used commonly in doses up to 50 mg/kg to induce preterm delivery.[23] However, on E15.5, we used a subclinical bolus dose of LPS (0.3 mg/kg) to determine whether HFD potentiates the effects of LPS. Our results indicate that HFD consumption significantly increases the number of dams that deliver within 24 hours (after E15.5 LPS) compared with NCD mice (Figure 4). Surprisingly, LPS priming completely protected HFD mice (n=7) from preterm delivery. Whereas most HFD mice (n=13) delivered within 48 hours (after E15.5 LPS), none of the HFD-LPS–primed mice delivered before E19 of gestation (Figure 4). Day E19 reflects a normal, term delivery in mice; the range for term delivery is from E19–E21. Further, this effect was significantly greater in HFD mice and LPS priming had no statistically significant effect on NCD mice.

HFD-LPS–primed mice have increased circulating levels of progesterone

To determine the circulating levels of progesterone, we performed cardiac puncture after dams delivered their first pups and collected sera from NCD, HFD, and HFD-LPS–primed mice. The HFD-LPS–primed mice had greater circulating progesterone levels compared with NCD and HFD mice (Figure 5, A). This finding suggests that the protective effects of LPS priming may be due to increased levels of circulating progesterone.

HFD-LPS–primed mice have increased antioxidant and antiinflammatory capacity

We performed cardiac puncture after dams delivered their first pups and collected sera from NCD, HFD, and HFD-LPS–primed mice to assess the host oxidative stress response. HFD mice have a significantly diminished total antioxidant capacity compared with NCD mice ($P<.05$), and LPS priming significantly increases the antioxidant capacity of HFD mice compared with mice that consume HFD alone ($P<.01$; Figure 5, B). To assess the heterogeneity of the oxidative stress

FIGURE 5
High-fat diet—lipopolysaccharide priming significantly increases progesterone levels, restores antioxidant capacity, and suppresses inflammation

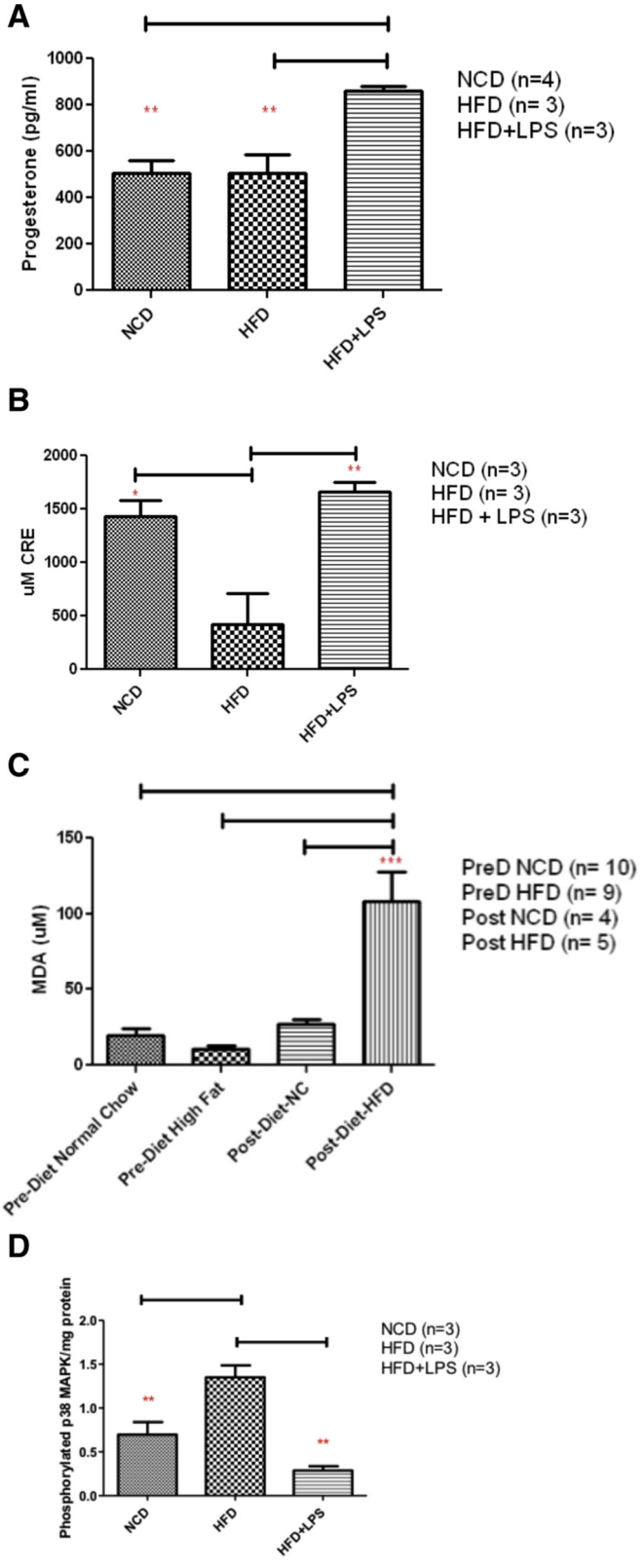

response between NCD and HFD mice, we collected urine samples before and after the 8-week diet regimen. We evaluated oxidative stress using a lipid peroxidation assay that measures the production of the lipid peroxidation product malondialdehyde. Our results indicated that HFD consumption significantly increases the level of malondialdehyde in urine compared with consumption of the NCD (Figure 5, C).

To determine the heterogeneity of the inflammatory-oxidative stress axis among NCD, HFD, and HFD-LPS–primed mice, we collected uteri after dams delivered their first pups and measured the activation of p38 MAPK. HFD consumption significantly increased the activation of p38 MAPK compared with NCD consumption ($P<.01$), and LPS priming decreased p38 MAPK activation ($P<.01$) in HFD mice compared with consumption of a HFD alone (Figure 5, D). Cumulatively, these results suggest that HFD consumption attenuates antioxidant capacity and increases inflammation and that HFD consumption with LPS priming significantly increases antioxidant capacity and suppresses the inflammatory response to LPS.

A, Circulating serum progesterone levels in normal control diet, high-fat diet, and high-fat diet—lipopolysaccharide-primed groups. **B,** Total antioxidant capacity, measured as copper-reducing equivalents, in normal control diet, high-fat diet, and high-fat diet—lipopolysaccharide-primed groups. **C,** Malondialdehyde levels in the urine of normal control diet and high-fat diet mice (before and after the 8-week diet regimen). **D,** Phosphorylated p38 mitogen activated protein kinase levels in normal control diet, high-fat diet, and high-fat diet—lipopolysaccharide-primed groups. *Bars* represent means±standard error of the mean. Statistical significance was determined with the use of Tukey's multiple comparison tests after 1-way analysis of variance. **A-C,** $^{**}P<.01$; $^{***}P<.001$; **D,** Newman-Keuls multiple comparison tests after analysis of variance.

CRE, copper-reducing equivalents; *HFD*, high-fat diet; *LPS*, lipopolysaccharide; *MDA*, malondialdehyde; *NC*, normal control diet.

Manuel et al. Immune tolerance decreases risk of preterm birth in high-fat diet mice. Am J Obstet Gynecol 2019.

FIGURE 6
Lipopolysaccharide priming partially restores the gut microbiome from high-fat diet–induced dysbiosis

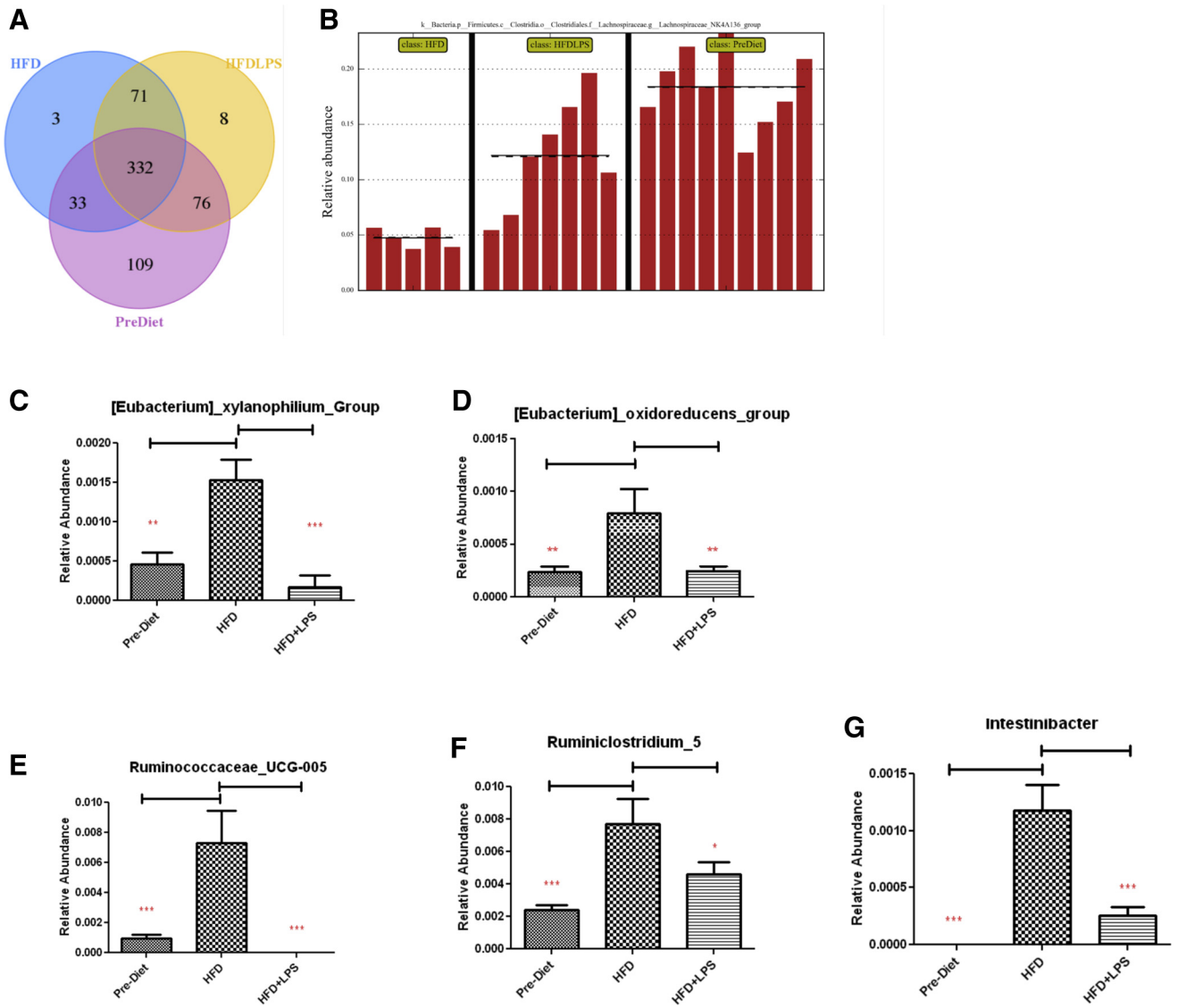

A, A representative operational taxonomic units—Venn graph of normal control diet (n=9), high-fat diet (n=4), and high-fat diet—lipopolysaccharide-primed (n=7) groups. Different groups are represented by different colors. The number in the overlapping areas that are shared by different color patterns is the number of operational taxonomic units that were shared by the groups, although the number in the nonoverlapping parts is the number of unique operational taxonomic units that are distinct to each of the different groups. **B,** A relative abundance histogram of *Lachnospiraceae_NK4A136_group* in high-fat diet, high-fat diet—lipopolysaccharide-primed, and normal control diet groups. Each *bar* represents the relative abundance for 1 mouse within each group. Statistical significance was determined by Tukey's multiple comparison test after 1-way analysis of variance (probability value for high-fat diet vs high-fat diet—lipopolysaccharide-primed=.0089004; probability value for high-fat diet vs normal control diet=.0000116; probability value for high-fat diet—lipopolysaccharide-primed vs normal control diet=.0111002). **C,** Relative abundance of *[Eubacterium]_xylanophillium_group* after high-fat diet consumption, compared with normal control diet and high-fat diet—lipopolysaccharide-primed groups. **D,** Relative abundance of *[Eubacterium]_oxidoreducens_group* after high-fat diet consumption, compared with normal control diet and high-fat diet—lipopolysaccharide-primed groups. **E,** Relative abundance of *Ruminococcaceae_UCG-005* after high-fat diet consumption, compared with normal control diet and high-fat diet—lipopolysaccharide-primed groups. **F,** Relative abundance of *Ruminiclostridium_5* after high-fat diet consumption, compared with normal control diet and high-fat diet—lipopolysaccharide-primed groups. **G,** Relative abundance of *Intestinibacter* after high-fat diet consumption, compared with normal control diet and high-fat diet—lipopolysaccharide-primed groups. **C–G,** *Bars* represent means±standard error of the mean. Statistical significance was determined by Tukey's multiple comparison test after 1-way analysis of variance (*$P<.05$; **$P<.01$; ***$P<.001$.

HFD, high-fat diet; *HFD+LPS*, high-fat diet—lipopolysaccharide-primed; *LPS*, lipopolysaccharide; *NCD*, normal control diet; *OTUs*, operational taxonomic units; *PreDiet*, normal control diet.

Manuel et al. Immune tolerance decreases risk of preterm birth in high-fat diet mice. Am J Obstet Gynecol 2019.

FIGURE 7
Normal control diet, high-fat diet, and high-fat diet—lipopolysaccharide mice have distinct metabolomic profiles

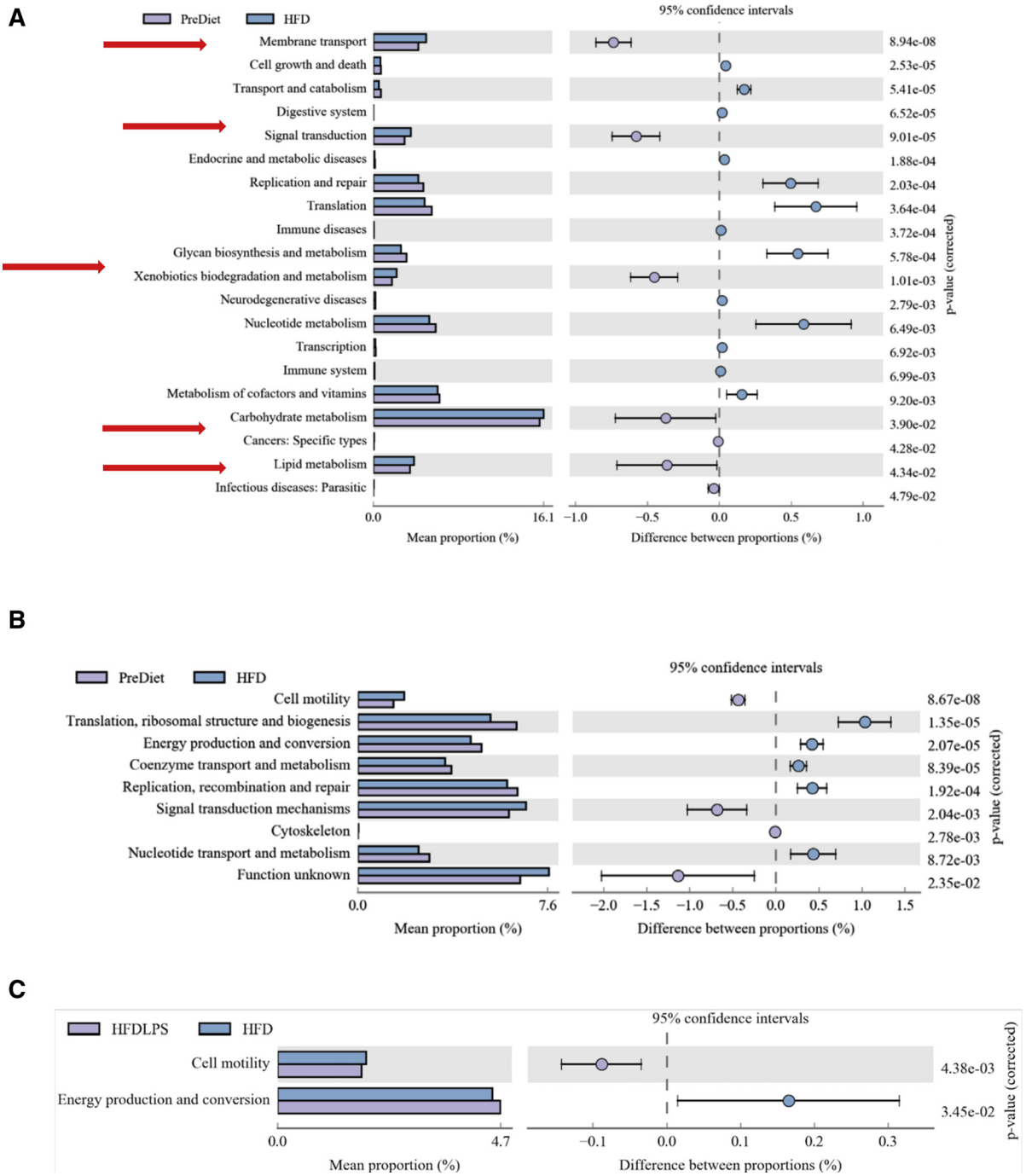

A, Kyoto Encyclopedia of Genes and Genomes metabolic pathway differential analysis of normal control diet (n=9) and high-fat diet groups. The *red arrows* indicate metabolic pathways that were increased significantly after high-fat diet consumption. Each *colored bar* represents a different group. **B,** A representative protein function classification chart with functional distribution and abundance between normal control diet and high-fat diet groups. **C,** Metabolic pathway differential analysis between high-fat diet (n=4) and high-fat diet—lipopolysaccharide-primed (n=7) groups. The data are represented as the mean proportion (percent) and difference between proportion (percent) within the normal control diet, high-fat diet, and high-fat diet—lipopolysaccharide-primed groups. G-test in Statistical Analysis of Metagenomic Profiles (large sample size: annotated functional gene number >20) and Fisher (small sample size: annotated functional gene number <20) were used for the species abundance at genus level to perform the significant difference test between 2 samples and *t*-test between 2 groups. The probability value threshold is .05.

HFD, high-fat diet; *HFDLPS*, high-fat diet—lipopolysaccharide-primed; *LPS*, lipopolysaccharide; *NCD*, normal control diet.

Manuel et al. Immune tolerance decreases risk of preterm birth in high-fat diet mice. Am J Obstet Gynecol 2019.

FIGURE 8
High-fat diet—lipopolysaccharide priming normalizes the uterine transcriptome

A

DEG Set	All DEG	up-regulated	down-regulated
Black_74_Red_91_Red_72_Black_93_Blue_90_vs_Black_36_Black_37_Green_35	77	51	26
Black_74_Red_91_Red_72_Black_93_Blue_90_vs_Green_40_Green_62_Blue_91_Red_95	994	610	384
Green_40_Green_62_Blue_91_Red_95_vs_Black_36_Black_37_Green_35	394	147	247

B **C**

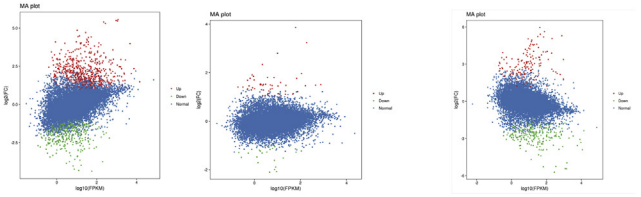

D **E**

Inflammation and Oxidative Stress	LPS-TLR4	Apoptosis/ Autophagy	Smooth Muscle Contraction	Inflammation and Oxidative Stress	LPS-TLR4	Apoptosis/ Autophagy	Smooth Muscle Contraction
Csf1	LBP, Marco	Prf1, Selp	Nts	Csf1, Stfa2	LBP, Marco	Prf1	Nts
Madcam1			Nucb2	Fcrl6, Madcam1		Dcn	Nucb2
Cxcl13, Cxcl5 Ccl2, Cxcl3				Cxcl13, Cxcl5 Ccl2, Cxcl3		Selp	
Il-6, Crp, Ptgs2, Ptges, Cysltr2, Spp1				Il-6, Crp, Ptgs2, Ptges, Cysltr2, Spp1			
Ptx3				Ptx3			
Gbp2				Gbp2			
Map3k6, Pdk4				Olr1, Nox4, Map3k6, Nos2, Pdk4			
Ppp1r15a				Orm1, Saa3, Saa1			
Hilpda				Ppp1r15a, Cd109			
				Hilpda			

F

Alox15	Alox15	Foxl2	Clca1	Ly86
Rnase6	Clu			Chodl
Ppp2r2b	Sit1			Cd8a
Clca1				60 Igkvs (immunoglobulin kappa variable clusters). 19 clusters of genes were originally down-regulated with HFD
Sit1				
Cd22				
Cd226				
Gbp2b				

A, Number of differentially expressed genes in each pairwise comparison. *Color* and *number* represent 1 mouse from each group. Black 74, Red 91, Red 72, Black 93, and Blue 90: normal control diet group (n=5). Green 40, Green 62, Blue 91, and Red 95: HFD group (n=4). Black 36, Black 37, and Green 35: high-fat diet—lipopolysaccharide-primed group (n=3). The 3 comparisons that are shown, in order, are normal control diet vs high-fat diet—lipopolysaccharide, normal control diet vs high-fat diet, and high-fat diet vs high-fat diet—lipopolysaccharide. **B,** Log ratio+mean average plot of differentially expressed genes of normal control diet vs high-fat diet and normal control diet vs high-fat diet—lipopolysaccharide-primed groups. In the **first panel**, *red dots* represent genes that are up-regulated in the high-fat diet group compared with the normal control diet group; *green dots* represent genes that are down-regulated in the high-fat diet group compared with the normal control diet group; *blue dots* represent genes that are not expressed differentially between the 2 groups. In the **second panel**, *red dots* represent genes that are up-regulated in the high-fat diet—lipopolysaccharide group compared with the normal control diet group; *green dots* represent genes that are down-regulated in the high-fat diet—lipopolysaccharide group compared with the normal control diet group; *blue dots* represent genes that are not expressed differentially between the 2 groups. **C,** Log ratio+mean average plot of differentially expressed genes between high-fat diet and high-fat diet—lipopolysaccharide-primed groups. *Red dots* represent genes that are up-regulated in the high-fat diet group compared with the high-fat diet—lipopolysaccharide group; *green dots* represent genes that are down-regulated in the high-fat diet group compared with the high-fat diet—lipopolysaccharide group; *blue dots* represent genes that are not expressed differentially between the 2 groups. **D,** Summary of significantly up-regulated genes after high-fat diet consumption. **E,** Summary of significantly down-regulated genes after high-fat diet—lipopolysaccharide priming. Genes *highlighted in red* originally were up-regulated after high-fat diet consumption alone. **F,** Summary of significantly up-regulated genes after high-fat diet—lipopolysaccharide priming. **D**—**F,** Genes *highlighted in red* originally were down-regulated after high-fat diet consumption alone. GeneCards Human Gene Database and UniProt were used to identify gene. Statistical significances in gene expression were determined with the use of the Student *t* test (*$P<.05$).

DEG, differentially expressed genes; *FC*, fold change; *HFD*, high-fat diet; *MA*, log ratio+mean average.

Manuel et al. Immune tolerance decreases risk of preterm birth in high-fat diet mice. Am J Obstet Gynecol 2019.

HFD-LPS priming partially restores the gut microbiome because of dysbiosis

To assess the maternal gut microbiome, we collected stool samples before and after the 8-week diet regimen and characterized the microbial environment using 16S RNA sequencing. The results indicated that mice that consume HFDs have less distinct bacteria (OTUs) in common with NCD mice, compared with HFD-LPS–primed mice. Whereas HFD mice have 33 OTUs in common with NCD mice, HFD-LPS–primed mice share 76 OTUs (Figure 6, A). Also, we compared the most abundant genera across NCD, HFD, and HFD-LPS–primed mice and determined that the relative abundance of *Lachnospiraceae* decreases from approximately 16% in NCD mice to 4% in HFD mice (Figure 6, B).

After priming HFD mice with LPS, the relative abundance of *Lachnospiraceae,* which have been shown to protect against infection and inflammation because of the production of butyrate,[24] increased from 4% to approximately 13% (Figure 6, B). In addition to reduced *Lachnospiraceae*, stool from HFD mice contained a significantly greater abundance of *Eubacterium xylanophillium*, *E oxidoreduens*, *Intestinibacter*, *Ruminococcaceae_UCG-005*, and *Ruminiclostridium_5* genera, compared with NCD and HFD-LPS–primed mice (Figure 6, C–G).

After sequencing, we characterized the functional genes in samples using Phylogenetic Investigation of Communities by Reconstruction of Unobserved States (PICRUSt) software and analyzed the differences between functional genes of microbial communities using the Kyoto Encyclopedia of Genes and Genomes pathway analysis. To predict the protein function classification of these genes, we used Cluster of Orthologous Group family information. Figure 7 gives a comparison of gene expression between 2 groups. The greater the distance between the confidence intervals and the mean the greater the difference in the expression of that particular gene family in the 2 groups. Our results indicated that HFD mice have a significantly greater proportion of genes involved in membrane transport, signal transduction, xenobiotic biodegradation, carbohydrate/lipid metabolism, and cell motility compared with NCD mice (Figure 7, A and B). Furthermore, we show that LPS priming significantly decreases the proportion of genes that are involved in cell motility and significantly increases the proportion of genes that are involved in energy production/conversion compared with HFD consumption alone (Figure 7, C).

HFD-LPS priming normalizes the uterine transcriptome

To further explore the reason that LPS priming protects HFD mice from preterm delivery, we performed RNA transcriptome sequencing of uteri from NCD, HFD, and HFD-LPS–primed groups. Our results indicate that LPS priming significantly increases circulating progesterone (Figure 5, A) and down-regulates the expression of messenger RNAs that are involved in inflammation/oxidative stress, apoptosis/autophagy, and myometrial contraction (Figure 8, E). Also, LPS priming significantly up-regulated the expression of messenger RNAs that produce genes that are involved in immunoglobulin production, antimicrobial activity, and maintenance of pregnancy (Figure 8, F). Interestingly, NCD and HFD mice had 994 DEGs, whereas NCD and HFD-LPS–primed mice had only 77 DEGs (Figure 8, A). These results suggest that LPS priming normalizes the uterus transcriptome in HFD mice. This normalizing effect of LPS priming is illustrated further in Figure 8, B, where the obvious differences in gene expression between the NCD and HFD mouse uterine transcriptomes (shown in the first panel) almost disappear when the same comparison is made between NCD mice and HFD-LPS mice (shown in the second panel). The effect of LPS priming on gene expression is shown in Figure 8, C, which illustrates differential gene expression between the HFD and HFD-LPS transcriptomes. The majority of the genes up-regulated in HFD mice, as compared with NCD mice, not surprisingly, encode proteins that are related to inflammation and oxidative stress (Figure 8, D). LPS priming significantly reversed the effect of the HFD on the uterine transcriptome. In Figure 8, E, the names of genes down-regulated by LPS priming are listed. The genes originally up-regulated by HFD that were normalized by LPS priming are listed in red. Finally, in Figure 8, F, the names of genes up-regulated by LPS priming are listed. The genes originally down-regulated by HFD that were normalized by LPS priming are listed in red.

The significant effect of LPS priming is also illustrated by volcano plots (Figure S1). The number of uterine DEGs in HFD mice, when compared with NCD mice (Figure S1, A), is significantly greater than the number of DEGs shown in the volcano plot that compares LPS–primed HFD mice with NCD mice (Figure S1, B). Finally, the reversal of the effect of HFD consumption on the number of DEGs by LPS priming is shown by cluster analysis (Figure S2). A complete list of genes in HFD mice uteri that were affected by LPS priming is provided in Table S1.

Comment

Recent studies indicate that maternal infection is not required for sPTB.[8] Sterile inflammation caused by environmental factors such as HFD consumption may induce the onset of labor.[8] Currently, >60% of all pregnancies in the United States are in women who are overweight or obese at conception.[25] Maternal adiposity is significantly correlated with an increased risk of essentially all maternal and fetal complications.[11-18] However, many investigators rely on infection-induced inflammation and progesterone experimental models to resolve the mechanisms of sPTB and identify novel therapeutics. These approaches underestimate the multifactorial nature of sPTB and do not address the reasons that certain populations of women (eg, African-American and obese/overweight women) are disproportionately at risk for sPTB.

To determine the mechanisms of HFD-mediated sPTB, we expanded the standard model of infection-induced PTB and developed a novel in vivo model to evaluate the reasons that prematernal HFD consumption and weight gain are correlated with sPTB. Although it has been previously shown that HFD-induced dysbiosis leads to activation of the TLR4 signaling pathway and inflammation in C57BL/6 mice,[26] we are the first to report that HFD in pregnant mice leads to sPTB via this mechanism. In our model, we assigned mice to either a NCD or HFD for 8 weeks. In this study, we show that chronic HFD consumption significantly increases the risk of sPTB and decreases fetal viability compared with NCD consumption. Although LPS is a well-known mediator of sPTB in murine models, our results unexpectedly indicated that LPS priming completely protects HFD dams from sPTB and does not have a statistically significant effect in NCD dams. Whereas most of the HFD dams delivered within 48 hours of the administration of LPS, HFD-LPS—primed mice challenged with the same dose of LPS delivered at term between E19 and E21. Our results suggest that LPS priming selectively protects HFD dams and pups from the adverse effects of endotoxin exposure. Although LPS priming also appears to protect NCD mice from sPTB, there is no significant difference between the onset time of delivery between NCD and LPS—primed NCD mice (Figure 6, A and B).

We show here, for the first time, that LPS priming protects HFD dams from sPTB by (1) increasing antioxidant capacity, (2) increasing circulating progesterone, and (3) normalizing the gut microbiome. Inflammation and oxidative stress mediate the onset of labor both regulating the production of contraction-associated proteins and decreasing circulating progesterone.[8,27] Although investigators have identified several potential mechanisms of inflammation-induced PTB, the mechanisms of oxidative stress—mediated PTB remain to be elucidated.[28] Recently, several studies reported that the inflammatory-oxidative stress axis, normally triggered in term labor, initiates senescence and aging of fetal tissues prematurely by activation of p38 MAPK.[29-32] Premature aging is correlated with sterile inflammation, which can initiate preterm labor or preterm premature rupture of membranes.[29-32]

Previous studies indicate that progesterone withdrawal from the circulation increases the production of inflammatory cytokines and chemokines and increases the production of contraction-associated proteins such as connexin in some mammals.[33,34] This disruption of immune tolerance creates an inflammatory, oxidative uteroplacental environment that changes the quiescent state of the uterus to an active state, leading to the onset of labor.[34-36] Increased circulating progesterone, on the other hand, decreases systemic inflammation and prevents sPTB.[37] Although its effect on circulating progesterone may play a part in the mechanism through which LPS priming prevents sPTB in our murine model, it is difficult to know whether this effect would translate to humans, because primates do not experience a precipitous drop in progesterone in pregnancy.

It is known widely that mutualistic microbes reside throughout the body.[38,39] Healthy gut microbiota have crucial functions in the host, such as development of the immune system, protection against opportunistic infections, facilitation of digestion, and production of bioactive metabolites.[40-44] Recently, it has been reported that alterations in the composition and function of gut microbiota (ie, dysbiosis) contribute to systemic inflammation and oxidative stress.[45-47] For example, chronic consumption of HFDs induces gut dysbiosis and activates the inflammatory-oxidative stress axis that predisposes individuals to obesity and metabolic disease.[48-51] In the context of PTB, studies have suggested that maternal gut, uteroplacental, or vaginal dysbiosis are significantly correlated with PTB and the onset of labor.[8,52-55] It should be noted that pregnant African-American women have a distinct vaginal microbiome that may contribute to their increased risk of spontaneous preterm delivery.[56,57]

Species within *Eubacterium*, which were increased in the HFD mice gut microbiomes, have been shown to increase resistance to *Clostridium difficile* infection and are associated with bacterial vaginosis.[58-,59] Bacterial vaginosis is the most common infection associated with PTB.[60-63] Bacterial species within *Intestinibacter*, *Ruminococcaceae*, and *Ruminiclostridium*, which also are increased by HFD, are correlated positively with inflammation, insulin resistance, dyslipidemia, and bacterial vaginosis and are resistant to oxidative stress.[64-69] The recovery of *Lachnospiraceae_NK4A136_group* and significant decrease in abundance of *Intestinibacter* after HFD-LPS priming suggests that part of the protection is due to butyrate production and suppression of acetate production. Recent studies show that butyrate has antiinflammatory properties and that acetate is a cervicovaginal risk factor of sPTB.[70-74] Also, a recent study reported that immunotherapy normalizes the gut microbiome and prevents type-1 diabetes mellitus.[75]

In addition to normalization of the gut microbiome, we show that HFD-LPS priming normalizes the uterus transcriptome by decreasing genes that are involved in the inflammatory-oxidative stress axis, autophagy/apoptosis, and smooth muscle contraction. HFD-LPS priming normalizes the uterus transcriptome by increasing Foxl2, a gene that is involved in the maintenance of pregnancy.[76,77] Our results indicate that LPS priming significantly decreases the expression of genes (ie, LBP and marco) that regulate TLR4 activation and response and significantly increases the expression of 61 genes that positively regulate immunoglobulin function and potentially mediate endotoxin tolerance.[78-83] We also show that LPS priming significantly decreases the expression of 14 genes that regulate sodium channel function. The activation of myometrial sodium channels could result in the release of endoplasmic reticulum stores of calcium that initiate contraction and the onset of labor.[84,85]

Cumulatively, our findings suggest that HFD consumption significantly potentiates low-grade inflammation and mediates sPTB. HFD consumption stimulates the inflammatory-oxidative stress axis systemically and the uterus and placenta locally. This stimulation drives dysbiosis of the gut microbiome that initiates a positive-feedback loop causing more inflammation and oxidative stress. The increased inflammation and oxidative stress in the uteroplacental environment subsequently stimulates premature delivery. Although a potential limitation of this study is the small size of some of the experimental groups, our results suggest that controlled production of immune tolerance may be a more targeted approach to inhibiting sPTB in overweight mothers or mothers with high-fat diets. Currently, 17-OHPC has been shown to lack efficacy in these populations. Thus, new personalized therapies are needed. Although LPS was used in this study in an experimental model, a bacterial extract without toxic properties could be chosen judiciously for administration to pregnant women to induce immune tolerance. *Lactobacillus plantarum*, a species of probiotic bacteria, or even butyrate could be tested for the potential to reverse the unfavorable effects of gut dysbiosis.

Clearly, novel progesterone analogs and antiinflammatory drugs are not appropriate treatments for all women who are at risk of sPTB. To decrease the incidence of sPTB significantly and to improve neonatal outcomes, we must expand our experimental models and incorporate some of the newly discovered noninfectious mediators of sPTB, such as socioeconomic status and demographic factors, smoking, and HFD consumption. These models will allow us to develop novel, personalized pharmacotherapy for women, such as African-American and overweight/obese women who are disproportionately at risk for sPTB. ■

Acknowledgments

We are grateful to Ms Helen Scaramell and the entire St. John's University Animal Care Center staff for assisting with timed matings and caring for the mice.

The authors declare no competing financial interests.

Author contributions: C.R.M. participated in the development of the hypotheses, designed many of the experiments, performed all of experiments and wrote the manuscript. M.S.L. analyzed the microbiome data. C.R.A. provided intellectual input in the development of the project and assisted with the presentation of the data and writing of the manuscript. S.E.R. provided the original idea for the project, assisted in the design of the experiments and supervised the experiments.

References

1. Glover AV, Manuck TA. Screening for spontaneous preterm birth and resultant therapies to reduce neonatal morbidity and mortality: a review. Semin Fetal Neonatal Med 2018;23:126–32.
2. Vogel JP, Chawanpaiboon S, Moller A-B, Watananirun K, Bonet M, Lumbiganon P. The global epidemiology of preterm birth. Best Prac Res Clin Obstet Gynaecol 2018;52:3–12.
3. Barfield WG. Public health implications of very preterm birth. Clin Perinatol 2018;45:565–77.
4. Timofeev J, Singh J, Istwan N, Rhea R, Driggers RW. Spontaneous preterm birth in African-American and caucasian women receiving 17α-hydroxyprogesterone caproate. Am J Perinatol 2014;31:55–60.
5. Manuel CR, Ashby CR, Reznik SE. Discrepanices in animal models of preterm birth. Curr. Pharm. Des 2017;23:6142–8.
6. Mohamed SA, Thota C, Browne PC, Diamond MP, Al-Hendy A. 2015. Why is preterm birth stubbornly higher in African-Americans? Obstet Gynecol Internat J 2014:1.
7. Chen C, Xu X, Yan Y. 2018. Estimated global overweight and obesity burden in pregnant women based on panel data model. PLoS One 2018;13:e0202183.
8. Keelan JA. Intrauterine inflammatory activation, functional progesterone withdrawal, and the timing of term and preterm birth. J Reprod Immunol 2017;125:89–99.
9. Salomon C, Nuzhat Z, Dixon CL, Menon R. Placental exosomes during gestation: liquid biopsies carrying signals for the regulation of human parturition. Curr Pharm Des 2018;24:974–82.
10. Son KA, Kim M, Kim YM, et al. Prevalence of vaginal microorganisms among pregnant women according to trimester and association with preterm birth. Obstet Gynecol Sci 2018;61:38–47.
11. Grieger J, Grzeskowiak LE, Clifton VL. Preconception dietary patterns in human pregnancies are associated with preterm delivery. J Nutr 2014;144:1075–80.
12. Martin C, Sotres-Alvarez D, Siega-Riz AM. Maternal dietary patterns during the second trimester are associated with preterm birth. J Nutr 2015;145:1857–64.
13. Smith LK, Draper ES, Evans TA, et al. Associations between late and moderately preterm birth and smoking, alcohol, drug use and diet: a population-based case-cohort study. Arch Dis Chil Fetal Neonatal Ed 2015;100:F486–91.
14. Chia AR, de Seymour JV, Colega M, et al. A vegetable, fruit, and white rice dietary pattern during pregnancy is associated with a lower risk of preterm birth and larger birth size in a multiethnic Asian cohort: the Growing Up in Singapore Towards healthy Outcomes (GUSTO) cohort study. Am J Clin Nutr 2016;10:1416–23.
15. Zerfu T, Umeta M, Baye K. Dietary diversity during pregnancy is associated with reduced risk of maternal anemia, preterm delivery, and low birth weight in a prospective cohort study in rural Ethiopia. Am J Clin Nutr 2016;103:1482–8.
16. Brantsæter A, Englund-Ögge L, Haugen M, et al. Maternal intake of seafood and supplementary long chain n-3 poly-unsaturated fatty acids and preterm delivery. BMC Pregnancy Childbirth 2017;17:41.
17. Englund-Ögge L, Birgisdottir BE, Sengpiel V, et al. Meal frequency patterns and glycemic properties of maternal diet in relation to preterm delivery: results from a large prospective cohort study. PLoS One 2017;12:e0172896.
18. Zhang Y, Zhou H, Perkins A, Wang Y, Sun J. Maternal dietary nutrient intake and its association with preterm birth: a case-control study in Beijing, China. Nutrients 2017;9.
19. Ingalls RH, Heine H, Lien E, Yoshimura A, Golenbock D. Lipopolysaccharide recognition, CD14, and lipopolysaccharide receptors. Infect Dis Clinics North Am 1999;13:341–53.
20. Noguchi T, Sado T, Naruse K, et al. Evidence for activation of Toll-like receptor and receptor for advanced glycation end products in preterm birth. Mediators Inflamm 2010;2010:490406.
21. Thaxton J, Nevers TA, Sharma S. TLR-mediated preterm birth in response to pathogenic agents. Infect Dis Obstet Gynecol 2010. https://doi.org/10.1155/2010/378472 [Epub ahead of print.].
22. Cappelletti M, Della BS, Ferrazzi E, Mavilio D, Divanovic S. Inflammation and preterm birth. J Leukocyte Biol 2016;99:67–78.
23. Sundaram S, Ashby CR, Pekson R, et al. N-dimethylacetamide regulates the proinflammatory response associated with endotoxin and prevents preterm birth. Am J Pathol 2013;183:422–30.
24. Borton MA, Sabag-Daigle A, Wu J, et al. Chemical and pathogen-induced inflammation disrupt the murine intestinal microbiome. Microbiome 2017;5:1.
25. Saben J, Lindsey F, Zhong Y, et al. Maternal obesity is associated with a lipotoxic placental environment. Placenta 2014;35:171–7.
26. Kim K-A, Wan G, Lee I-A, Joh E-H, Kim D-H. High-fat diet induced gut microbiota exacerbates inflammation and obesity in mice via the TLR4 signaling pathway. PLoS One 2012;7:e47713.

27. Behnia F, Sheller S, Menon R. Mechanistic differences leading to infectious and sterile inflammation. Am J Reprod Immunol 2016;75:505–18.

28. Menon R. Oxidative stress damage as a detrimental factor in preterm birth pathology. Front Immunol 2014;5:567.

29. Dutta EH, Behnia F, Boldogh I, et al. Oxidative stress damage-associated molecular signaling pathways differentiate spontaneous preterm birth and preterm premature rupture of the membranes. Mol Hum Reprod 2016;22:143–57.

30. Menon R, Papaconstantinou J. p38 Mitogen activated protein kinase (MAPK): a new therapeutic target for reducing the risk of adverse pregnancy outcomes. Expert Opin Ther Targets 2016;20:1397–412.

31. Menon R, Behnia F, Polettini J, Saade GR, Campisi M, Verlarde M. Placental membrane aging and HMGB1 signaling associated with human parturition. Aging 2016;8:216–30.

32. Dixon C, Richardson L, Sheller-Miller S, Saade G, Menon R. A distinct mechanism of senescence activation in amnion epithelial cells by infection, inflammation, and oxidative stress. Am J Reprod Immunol 2018;79:e12790.

33. Manuck T. 17-alpha hydroxyprogesterone caproate for preterm birth prevention: Where have we been, how did we get here, and where are we going? Semin Perinatol 2017;41:461–7.

34. Sivarajasingam S, Imami N, Johnson MR. Myometrial cytokines and their role in the onset of labour. J Endocrinol 2016;231:R101–19.

35. Schumacher A, Costa SD, Zenclussen AD. Endocrine factors modulating immune responses in pregnancy. Front Immunol 2014;5:196.

36. Nair R, Verma P, Singh K. Immune-endocrine crosstalk during pregnancy. Gen Comp Endocrinol 2017;242:18–23.

37. Weatherborn M, Mesiano S. Rationale for current and future progestin based therapies to prevent preterm birth. Best Prac Res Clin Obstet Gynaecol 2018;52:114–25.

38. Gouba N, Drancourt M. Digestive tract mycobiota: a source of infection. Med Mal Infect 2015;45:9–16.

39. Slocum C, Kramer C, Genco CA. Immune dysregulation mediated by the oral microbiome: potential link to chronic inflammation and atherosclerosis. J Intern Med 2016;280:114–28.

40. Stecher B, Hardt WD. The role of microbiota in infectious disease. Trends Microbiol 2008;16:107–14.

41. Patterso E, Cryan JF, Fitzgerald GF, Ross RP, Dinan TG, Stanton C. Gut microbiota, the pharmabiotics they produce and host health. Proc Nutr Soc 2014;73:477–89.

42. Schubert AM, Rogers MA, Ring C, et al. Microbiome data distinguish patients with Clostridium difficile infection and non-C. difficile-associated diarrhea from healthy controls. mBio 2014;5:01021-14.

43. Picchianti-Diamanti A, Rosado MM, D'Amelio R. Infectious agents and inflammation: The role of microbiota in autoimmune arthritis. Front Microbiol 2018;8:2696.

44. Yang H, Duan Z. The local defender and functional mediator: gut microbiome. Digestion 2018;97:137–45.

45. Laugerette F, Vors C, Peretti N, Michalski MC. Complex links between dietary lipids, endogenous endotoxins and metabolic inflammation. Biochim 2011'93:39–45.

46. Myles I. Fast food fever: reviewing the impacts of the Western diet on immunity. Nutr J 2014;13:61.

47. Mahmoodpoor F, Rahbar Saadat Y, Barzegari A, Ardalan M, Zununi Vahed S. The impact of gut microbiota on kidney function and pathogenesis. Biomed Pharmacother 2017;93:412–9.

48. Brandsma E, Houben T, Fu J, Shiri-Sverdlov R, Hofker MH. The immunity-diet-microbiota axis in the development of metabolic syndrome. Curr Opin Lipid 2015;26:2.

49. Murphy E, Velazquez KT, Herbert KM. Influence of high-fat diet on gut microbiota: a driving force for chronic disease risk. Curr Opin Clin Nutr Metab Care 2015;18:515–20.

50. Tomas J, Mulet C, Saffarian A, et al. High-fat diet modifies the PPAR-γ pathway leading to disruption of microbial and physiological ecosystem in murine small intestine. Proc Nat; Acad Sci U S A 2016;113:E5934–43.

51. Martinez K, Leone V, Chang EB. Western diets, gut dysbiosis, and metabolic diseases: Are they linked? Gut Microbes 2017;8:130–42.

52. Fox C, Eichelberger K. Maternal microbiome and pregnancy outcomes. Fertil Steril 2015;104:1358–63.

53. Prince AL, Chu DM, Seferovic MD, Antony KM, Ma J, Aargaard KM. The perinatal microbiome and pregnancy: moving beyond the vaginal microbiome. Cold Spring Harb Perspect Med 2015;5:6.

54. Prince AL, Ma J, Kannan PS, et al. The placental membrane microbiome is altered among subjects with spontaneous preterm birth with and without chorioamnionitis. Am J Obstet Gynecol 2016;214:627.e1–16.

55. Vinturache A, Gwamfi-Bannerman C, Hwang J, Misorekar IU, Jacobbson B, and The Preterm Birth International Collaborative. Maternal microbiome: a pathway to preterm birth. Semin Fetal Neonatal Med 2016;21:94–9.

56. Fettweis JM, Brooks JP, Serrano MG, et al. Differences in vaginal microbiome in African American women versus women of European ancestry. Microbiology 2014;160:2272–82.

57. Nelson D, Shin H, Wu J, Dominguez-Bello MG. The gestational vaginal microbiome and spontaneous preterm birth among nulliparous African American women. Am J Perinatol 2016;33:887–93.

58. Africa C, Nel J, Stemmet M. Anaerobes and bacterial vaginosis in pregnancy: Virulence factors contributing to vaginal colonisation. Int J Environ Res Public Health 2014;11:6979–7000.

59. Vincent C, Miller MA, Edens TJ, Mehrotra S, Dewar K, Manges AR. Bloom and bust: intestinal microbiota dynamics in response to hospital exposures and Clostridium difficile colonization or infection. Microbiome 2016;4:12.

60. Meis PJ, Goldenberg RL, Mercer B, et al. The preterm prediction study: Significance of vaginal infections. Am J Obstet Gynecol 1995;174:1231–5.

61. Leitich H, Bodner-Adler B, Brunbauer M, Kaider A, Egarter C, Husslein P. Bacterial vaginosis as a risk factor for preterm delivery: a meta-analysis. Am J Obstet Gynecol 2003;189:139–47.

62. Klebanoff M, SHillier S, Nugent RP, et al. Is bacterial vaginosis a stronger risk factor for preterm birth when it is diagnosed earlier in gestation? Am J Obstet Gynecol 2005;192:470–7.

63. Haahr T, Ersbøll AS, Karlsen NA, et al. Treatment of bacterial vaginosis in pregnancy in order to reduce the risk of spontaneous preterm delivery: a clinical recommendation. Acta Obstet Gynecol Scand 2016;95:850–60.

64. Romero R, Hassan SS, Gajer P, et al. The composition and stability of the vaginal microbiota of normal pregnant women is different from that of non-pregnant women. Microbiome 2014;2:1.

65. Davey L, Halperin SA, Lee SF. Thiol-disulfide exchange in Gram positive firmicutes. Trends Microbiol 2016;24:902–15.

66. Gomez-Arango LF, Barrett HL, McIntyre HD, Callaway LI, Morrison M, Nitert MD. Connections between the gut microbiome and metabolic hormones in early pregnancy in overweight and obese women. Diabetes 2016;65:2214–23.

67. Jotham S, Shapiro H, Elinav E. Role of the microbiome in the normal and aberrant glycemic response. Clin Nutr Exper 2016;6:59–73.

68. Dumitrache A, Klingeman DM, Natzke J, et al. Specialized activities and expression differences for Clostridium thermocellum biofilm and planktonic cells. Sci Rep 2017;7:43583.

69. Kuang Y-S, JLu J-H, Li S-H, et al. Connections between the human gut microbiome and gestational diabetes mellitus. Gigascience 2017;6:1–12.

70. Reeves A, Koenigsknecht MJ, Bergin IL, Young VB. Suppression of Clostridium difficile in the gastrointestinal tracts of germfree mice inoculated with a murine isolate from the family Lachnospiraceae. Infect Immunol 2012;80:3786–94.

71. Pérez-Cobas A, Moya A, Gosalbes MJ, Latorre A. Colonization resistance of the gut microbiota against Clostridium difficile. Antibiotics 2015;4:337–57.

72. Borton MA, Sabag-Daigle A, Wu J, et al. Chemical and pathogen-induced inflammation disrupt the murine intestinal microbiome. Microbiome 2017;5:1.

73. Vital M, Karch A, Pieper DH. Colonic butyrate-producing communities in humans: an overview using omics data. mSystems 2017;2:6.

74. Amabebe E, Reynolds S, Stern V, Stafford G, Paley M, Anumba DOC. Cervicovaginal fluid acetate: a metabolite marker of preterm birth in symptomatic pregnant women. Front Med 2016;3:48.
75. Mullaney JA, Stephens JE, Costello M-E, et al. Type 1 diabetes susceptibility alleles are associated with distinct alterations in the gut microbiota. Microbiome 2018;6:1.
76. Uhlenhaut N, Treier M. Foxl2 function in ovarian development. Mol Genet Metab 2006;88:225–34.
77. Bellessort B, Bachelot A, Heude E, et al. Role of Foxl2 in uterine maturation and function. Hum Mol Genet 2015;24:3092–103.
78. Redegeld F, Nijkamp FP. Immunoglobulin free light chains and mast cells: pivotal role in T-cell-mediated immune reactions? Trends Immunol 2003;24:181–5.
79. Chen Y, Wermeling F, Sundqvist J, et al. A regulatory role for macrophage class A scavenger receptors in TLR4-mediated LPS responses. Eur J Immunol 2010;40:1451–60.
80. Ghosh S, Gregory D, Smith A, Kobzik L. MARCO regulates early inflammatory responses against influenza: a useful macrophage function with adverse outcome. Am J Respir Cell Mol Biol 2011;45:1036–44.
81. Groot KT, Askenase PW, Redegeld FA. Immunobiology of antigen-specific immunoglobulin free light chains in chronic inflammatory diseases. Curr Pharm Des 2012;18:2278–89.
82. Peri F, Piazza M. Therapeutic targeting of innate immunity with Toll-like receptor 4 (TLR4) antagonists. Biotech Adv 2012;30:251–60.
83. Park B, Lee JO. Recognition of lipopolysaccharide pattern by TLR4 complexes. Exp Mol Med 2013;45:e66.
84. Boyle M, Heslip LA. Voltage-dependent Na+ channel mRNA expression in pregnant myometrium. Receptors Channels 1994;2:249–53.
85. Choi K, An BS, Yang H, Jeung EB. Regulation and molecular mechanisms of calcium transport genes: do they play a role in calcium transport in the uterine endometrium? J Physiol Pharmacol 2011;62:499–504.

Author and article information

From the Department of Pathology and Cell Biology, Columbia University Medical Center, New York, NY (Dr Manuel); Department of Pediatrics, Albert Einstein College of Medicine, Bronx, NY (Dr Latuga); Department of Pharmaceutical Sciences, St John's University, Queens, NY (Drs Ashby Jr and Reznik); and the Departments of Pathology and Obstetrics and Gynecology and Women's Health, Albert Einstein College of Medicine, Bronx, NY (Dr. Reznik).

Received Oct. 12, 2018; revised Feb. 9, 2019; accepted Feb. 14, 2019.

Supported by a fellowship grant by the American Foundation for Pharmaceutical Education (C.R.M.) and St. John's University Seed Grants (S.E.R.).

The authors report no conflict of interest.

Corresponding author: Sandra E. Reznik, MD, PhD. rezniks@stjohns.edu

FIGURE S1

Volcano plots of differentially expressed genes from normal control mice vs high-fat diet and normal control mice vs high-fat diet—lipopolysaccharide-primed mice

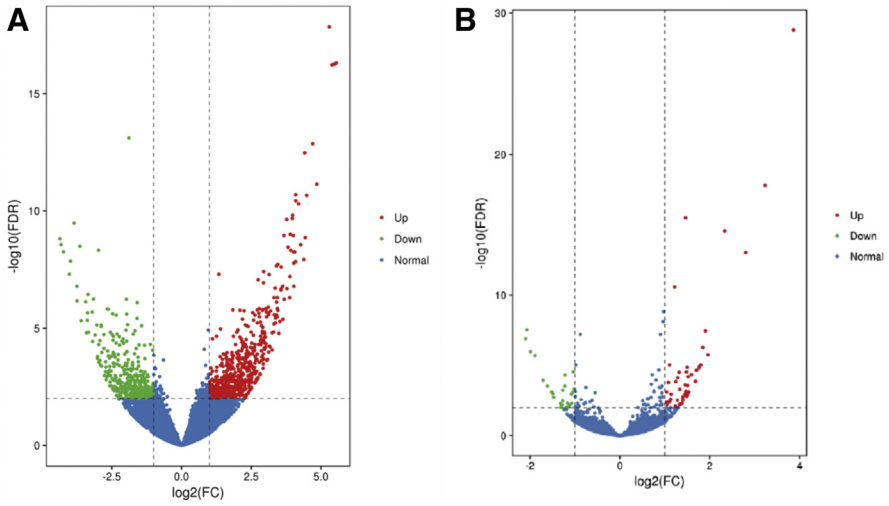

A, In the first panel, *red dots* represent genes that are up-regulated in the high-fat diet group as compared with the normal control diet group; *green dots* represent genes that are down-regulated in the high-fat diet group compared with the normal control diet group; *blue dots* represent genes that not differentially expressed between the 2 groups. **B,** In the second panel, *red dots* represent genes that are up-regulated in the high-fat diet—lipopolysaccharide group as compared with the normal control diet group; *green dots* represent genes that are down-regulated in the high-fat diet—lipopolysaccharide group compared with the normal control diet group; *blue dots* represent genes that are not differentially expressed between the 2 groups.

FC, fold change; *FDR*, false discovery rate.

Manuel et al. Immune tolerance decreases risk of preterm birth in high-fat diet mice. Am J Obstet Gynecol 2019.

FIGURE S2

Cluster analysis of differentially expressed genes from normal control diet vs high-fat diet mice and normal control diet vs high-fat diet—lipopolysaccharide-primed mice

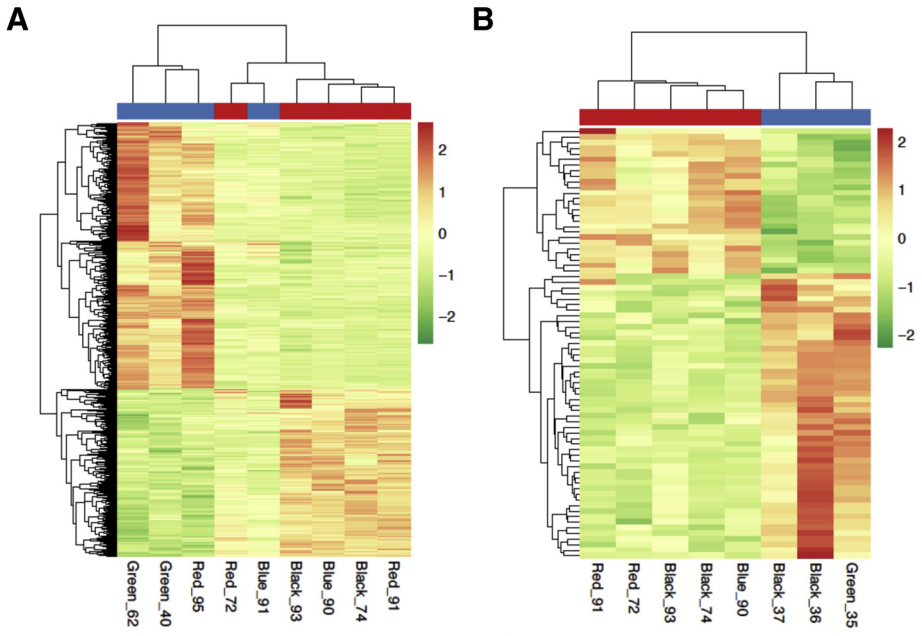

Hierarchic clustering based on fragments per kilobase of transcript per million mapped reads, where log2(fragments per kilobase of transcript per million mapped reads) is used for clustering. *Red color* represents genes with higher expression; *green color* represents genes with lower expression. Different columns represent different samples; different rows represent different genes. **A,** Cluster analysis: Black_74, Red_91, Blue_90, Black_93_Red_72 (normal control diet: 5); Blue_91, Red_95, Green_40, Green_62 (high-fat diet: 4). **B,** Cluster analysis: Black_74, Red_91, Blue_90, Black_93_Red_72 (normal control diet: 5); Black_36, Black_37, Green_35 (high-fat diet—lipopolysaccharide: 3).

Manuel et al. Immune tolerance decreases risk of preterm birth in high-fat diet mice. Am J Obstet Gynecol 2019.

TABLE S1
Total differentially expressed genes from high-fat diet vs high-fat diet–lipopolysaccharide-primed mice

Gene name	Up- or down-regulated
Clec10a	Up
Egfl6	Up
Car4	Down
Slc13a2	Down
Timp1	Down
Folr1	Down
Aif1l	Down
Cd3g	Up
Napsa	Down
Pla1a	Down
Ier3	Down
Pgf	Down
Apoa2	Down
Itih1	Down
Cyp27b1	Down
Sod2	Down
Klk4	Down
Ceacam5	Down
Cd163	Down
Slc5a1	Down
Pinlyp	Down
Cdh23	Down
Podnl1	Up
B4galnt2	Down
Csf1	Down
Cd48	Up
Gzmb	Down
Gzmf	Down
Lbp	Down
Hsd11b1	Down
Slpi	Down
Gpx3	Down
Slc13a3	Down
Adora2b	Down
Sfrp5	Down
Alox15	Up
Pdk4	Down
Popdc3	Down

Manuel et al. Immune tolerance decreases risk of preterm birth in high-fat diet mice. Am J Obstet Gynecol 2019.

(continued)

TABLE S1
Total differentially expressed genes from high-fat diet vs high-fat diet–lipopolysaccharide-primed mice *(continued)*

Gene name	Up- or down-regulated
Nts	Down
Dcn	Down
Slc5a8	Down
Srgn	Down
Irak3	Down
Madcam1	Down
Gfpt2	Down
Rrm2	Down
Nos2	Down
Coch	Down
Serpina3n	Down
Rdh12	Down
Akr1c18	Down
Net1	Down
Hhipl1	Down
Slc25a29	Down
Tnfaip2	Down
Slc17a4	Down
Prl7d1	Down
Serpinb9b	Down
Ly86	Up
Msx2	Up
Nkd2	Up
Rnase6	Up
Rgcc	Down
Scara5	Down
Clu	Up
Gzme	Down
Mcpt8	Down
Tgm1	Down
Ciita	Up
Apod	Down
Gpihbp1	Down
Ly6f	Down
Chodl	Up
Fetub	Down
Masp1	Down
Stfa2	Down

Manuel et al. Immune tolerance decreases risk of preterm birth in high-fat diet mice. Am J Obstet Gynecol 2019. *(continued)*

TABLE S1
Total differentially expressed genes from high-fat diet vs high-fat diet—lipopolysaccharide-primed mice *(continued)*

Gene name	Up- or down-regulated
Rcan1	Down
Cxcl13	Down
Serping1	Down
Cd4	Up
Clic5	Down
Tff1	Down
Cryaa	Down
Cyp1b1	Down
Prss28	Down
Fkbp5	Down
Ppp2r2b	Up
Cd74	Up
Scgb1a1	Down
Fosl1	Down
Rbp4	Down
Cbr2	Up
Cd7	Up
Tac2	Down
Avil	Down
Cdhr5	Down
Col7a1	Up
Il6	Down
Il18r1	Up
Il1r2	Down
Htr2b	Down
Marco	Down
Ppfia4	Up
Selp	Down
Slc43a3	Down
Gatm	Down
Angpt4	Down
Lrrc34	Down
Postn	Down
Ptx3	Down
Tchhl1	Down
Tdo2	Down
Ctsk	Down
Calb1	Up

Manuel et al. Immune tolerance decreases risk of preterm birth in high-fat diet mice. Am J Obstet Gynecol 2019. *(continued)*

TABLE S1
Total differentially expressed genes from high-fat diet vs high-fat diet—lipopolysaccharide-primed mice *(continued)*

Gene name	Up- or down-regulated
Atp6v0d2	Down
Clca1	Up
Gbp2	Down
Slc46a2	Down
Sit1	Up
Pdpn	Down
Slc2a1	Down
Map3k6	Down
Tnfrsf9	Down
Errfi1	Down
Abcb1b	Down
Htra3	Down
Spp1	Down
Slc10a6	Down
Alb	Down
Cxcl5	Down
Ereg	Down
Cxcl3	Down
Tfpi2	Down
Npy	Down
Wnt7a	Up
Slc6a12	Down
Klrg1	Down
Tuba8	Down
Olr1	Down
Wnt5b	Up
Rho	Down
Nox4	Down
Cd22	Up
Art2b	Up
Nucb2	Down
Calca	Down
Lat	Up
Aqp8	Down
Lyve1	Down
Adm	Down
Slc6a14	Down
Syt8	Up

Manuel et al. Immune tolerance decreases risk of preterm birth in high-fat diet mice. Am J Obstet Gynecol 2019. *(continued)*

TABLE S1
Total differentially expressed genes from high-fat diet vs high-fat diet—lipopolysaccharide-primed mice *(continued)*

Gene name	Up- or down-regulated
Gla	Down
Acsl4	Down
Asb11	Down
Myom2	Down
Asb5	Down
Fgfr1	Down
Hp	Down
Mt2	Down
Mt1	Down
Tmed6	Down
Trim29	Down
Cryab	Down
Cd3e	Up
Cd3d	Up
Cyp11a1	Down
Stra6	Up
Ptgs2	Down
Bmp8a	Down
Lama1	Up
Rspo4	Down
Itgbl1	Down
Guca2b	Down
Mgll	Down
AA467197	Down
Cysltr2	Down
Fgg	Down
Cd226	Up
Prss29	Down
Foxj1	Up
Ccl2	Down
Arhgap45	Up
Slc18a1	Down
Rnf39	Down
Card11	Up
H2-Aa	Up
Mgarp	Down
Prf1	Down
Map4k1	Up

Manuel et al. Immune tolerance decreases risk of preterm birth in high-fat diet mice. Am J Obstet Gynecol 2019. *(continued)*

TABLE S1
Total differentially expressed genes from high-fat diet vs high-fat diet—lipopolysaccharide-primed mice *(continued)*

Gene name	Up- or down-regulated
Serpine1	Down
Erv3	Down
Cldn11	Down
H2-DMa	Up
Themis2	Up
Crp	Down
Anpep	Up
Orm1	Down
Tgfb2	Down
Gimap3	Up
Cntnap2	Up
Clec10a	Down
Egfl7	Down
Car5	Down
Slc13a3	Up
Timp2	Up
Folr2	Down
Aif1l	Down
Cd3g	Down
Napsa	Down
Pla1a	Down
Clec10a	Down
Egfl7	Down
Car5	Down
Slc13a3	Up
Timp2	Down
Folr2	Down
Aif1l	Down
Cd3g	Down
Napsa	Down
Pla1a	Down
Ier4	Down
Pgf	Up
Apoa3	Down
Itih2	Down
Cyp27b2	Down
Sod3	Down
Klk5	Down

Manuel et al. Immune tolerance decreases risk of preterm birth in high-fat diet mice. Am J Obstet Gynecol 2019. *(continued)*

TABLE S1
Total differentially expressed genes from high-fat diet vs high-fat diet—lipopolysaccharide-primed mice *(continued)*

Gene name	Up- or down-regulated
Clec10a	Down
Egfl7	Up
Car5	Up
Slc13a3	Down
Timp2	Down
Folr2	Down
Aif1l	Up
Cd3g	Down
Napsa	Down
Pla1a	Up
Ier4	Up
Pgf	Up
Apoa3	Up
Itih2	Down
Cyp27b2	Down
Clec10a	Down
Egfl7	Up
Car5	Down
Slc13a3	Down
Timp2	Up
Folr2	Down
Aif1l	Down
Cd3g	Up
Napsa	Down
Pla1a	Down
Ier4	Up
Pgf	Down
Apoa3	Down
Itih2	Up
Cyp27b2	Down
Sod3	Down
Klk5	Down
Ceacam6	Down
Cd164	Up
Clec10a	Down
Egfl7	Up
Car5	Down
Slc13a3	Down

Manuel et al. Immune tolerance decreases risk of preterm birth in high-fat diet mice. Am J Obstet Gynecol 2019. *(continued)*

TABLE S1
Total differentially expressed genes from high-fat diet vs high-fat diet—lipopolysaccharide-primed mice *(continued)*

Gene name	Up- or down-regulated
Timp2	Down
Folr2	Down
Aif1l	Down
Cd3g	Down
Napsa	Down
Pla1a	Down
Ier4	Up
Pgf	Up
Apoa3	Up
Itih2	Down
Cyp27b2	Up
Sod3	Up
Klk5	Down
Ceacam6	Down
Cd164	Up
Slc5a2	Up
Pinlyp	Down
Cdh24	Down
Podnl2	Up
B4galnt3	Down
Csf2	Down
Cd49	Down
Gzmb	Up
Gzmf	Down
Lbp	Up
Hsd11b2	Up
Slpi	Down
Gpx4	Down
Slc13a4	Down
Adora2b	Down
Sfrp6	Down
Alox16	Down
Pdk5	Down
Popdc4	Up
Nts	Down
Dcn	Down
Slc5a9	Up
Srgn	Up

Manuel et al. Immune tolerance decreases risk of preterm birth in high-fat diet mice. Am J Obstet Gynecol 2019. *(continued)*

TABLE S1
Total differentially expressed genes from high-fat diet vs high-fat diet—lipopolysaccharide-primed mice *(continued)*

Gene name	Up- or down-regulated
Irak4	Up
Madcam2	Up
Gfpt3	Up
Rrm3	Up
Nos3	Up
Coch	Up
Serpina3n	Up
Rdh13	Up
Akr1c19	Up
Net2	Up
Hhipl2	Up
Slc25a30	Up
Tnfaip3	Up
Slc17a5	Up
Prl7d2	Up
Serpinb9b	Up
Ly87	Up
Msx3	Up
Nkd3	Up
Rnase7	Up
Rgcc	Up
Scara6	Down
Clu	Down
Gzme	Down
Mcpt9	Up
Tgm2	Up
Ciita	Up
Apod	Down
Gpihbp2	Down
Ly6f	Up
Chodl	Down
Fetub	Up
Masp2	Up
Stfa3	Up
Rcan2	Up
Cxcl14	Up
Serping2	Up
Cd5	Up

Manuel et al. Immune tolerance decreases risk of preterm birth in high-fat diet mice. Am J Obstet Gynecol 2019.

(continued)

TABLE S1
Total differentially expressed genes from high-fat diet vs high-fat diet–lipopolysaccharide-primed mice *(continued)*

Gene name	Up- or down-regulated
Clic6	Up
Tff2	Up
Cryaa	Up
Cyp1b2	Up
Prss29	Up
Fkbp6	Up
Ppp2r2b	Up
Cd75	Up
Scgb1a2	Up
Fosl2	Up
Rbp5	Up
Cbr3	Up
Cd8	Down
Tac3	Up
Avil	Up
Cdhr6	Up
Col7a2	Up
Il7	Up
Il18r2	Down
Il1r3	Up
Htr2b	Up
Marco	Up
Ppfia5	Up
Selp	Up
Slc43a4	Up
Gatm	Up
Angpt5	Up
Lrrc35	Up
Postn	Up
Ptx4	Up
Tchhl2	Up
Tdo3	Up
Ctsk	Up
Calb2	Down
Atp6v0d3	Up
Clca2	Down
Gbp3	Up
Slc46a3	Up

Manuel et al. Immune tolerance decreases risk of preterm birth in high-fat diet mice. Am J Obstet Gynecol 2019. *(continued)*

TABLE S1
Total differentially expressed genes from high-fat diet vs high-fat diet—lipopolysaccharide-primed mice *(continued)*

Gene name	Up- or down-regulated
Sit2	Down
Pdpn	Down
Slc2a2	Down
Map3k7	Down

Manuel et al. Immune tolerance decreases risk of preterm birth in high-fat diet mice. Am J Obstet Gynecol 2019.